A new microcirculation culture method with a self-organized capillary network

Kei Sugihara[1], Yoshimi Yamaguchi[1], Shiori Usui[1], Yuji Nashimoto[2–4], Sanshiro Hanada[5], Etsuko Kiyokawa[6], Akiyoshi Uemura[7], Ryuji Yokokawa[4], Koichi Nishiyama[5] and Takashi Miura[1]*

[1]Department of Anatomy and Cell Biology, Kyushu University Graduate School of Medical Sciences, Fukuoka 812-8582, Japan
[2]Frontier Research Institute for Interdisciplinary Sciences (FRIS), Tohoku University, Miyagi 980-8578, Japan
[3]Graduate School of Engineering, Tohoku University, Miyagi 980-8579, Japan
[4]Department of Micro Engineering, Kyoto University, Kyoto 615-8540, Japan
[5]International Research Center for Medical Sciences (IRCMS), Kumamoto University, Kumamoto 860-8556, Japan
[6]Department of Oncologic Pathology, Kanazawa Medical University, Ishikawa 920-0293, Japan
[7]Department of Retinal Vascular Biology, Nagoya City University Graduate School of Medical Sciences, Aichi 464-0083, Japan

Short title: A new microcirculation culture method

Corresponding author: Takashi Miura (miura_t@anat1.med.kyushu-u.ac.jp)

Abstract

A lack of microcirculation has been one of the most significant obstacles for three-dimensional culture systems of organoids and embryonic tissues. Here, we developed a simple and reliable method to implement a perfusable capillary network in vitro. The method employed the self-organization of endothelial cells to generate a capillary network and a static pressure difference for culture medium circulation, which can be easily introduced to standard biological laboratories and enables long-term cultivation of vascular structures. Using this culture system, we perfused the lumen of the self-organized capillary network and observed a flow-induced vascular remodeling process, cell shape changes, and collective cell migration. We also observed an increase in cell proliferation around the synthetic vasculature induced by flow, indicating functional perfusion of the culture medium. We also reconstructed extravasation of tumor and inflammatory cells, and circulation inside spheroids including endothelial cells and human lung fibroblasts. In conclusion, this system is a promising tool to elucidate the mechanisms of various biological processes related to vascular flow.

Introduction

Multicellular pattern formation has been one of the central issues in developmental biology [1–3]. An extensively used tool to understand the mechanism of pattern formation is an organ culture system in which embryonic tissue is cultured at the air-liquid interface [4]. Recent advancements in stem cell biology have enabled the generation of small tissue structures from a single cell, which is called an organoid, and various organoids have been established [5].

A technical obstacle for standard culture systems of three-dimensional tissue structures is the lack of microcirculation. There are various methods to improve oxygen supply, such as culture inserts and rotator culture [6]. However, these methods cannot overcome the size limitation, i.e., if the cultured tissue size exceeds a 100-μm order, the tissue undergoes necrosis due to hypoxia [7]. Reproduction of a functional capillary network has not been successful. For example, the tube formation assay has been classically used to assess the pattern formation capability of endothelial cells [8], but the generated network structure

57 lacks a functional lumen and is not perfusable.

58

59 Interactions between vascular endothelial cells and other types of cells are one of
60 the main themes of study in vascular biology. A major example is pericytes that
61 exist between basement membranes of endothelial cells, which stabilize the
62 biological activities of the endothelial cells [9]. In addition, endothelial cells
63 interact with circulating cells in blood [10]. For example, neutrophils transmigrate
64 through endothelial cells at an inflammation site [11]. In cancer biology,
65 hematogenous metastasis involves adhesion of tumor cells to endothelial cells and
66 invasion [12]. However, an effective in vitro system to observe these phenomena
67 is lacking.

68

69 In tissue engineering, various methods have been developed to implement a
70 capillary network in a microfluidic device for perfusion in culture systems [13].
71 These methods are classified into two categories: predesigned and self-
72 organization methods. Predesigned methods align endothelial cells by

73 engineering techniques. Self-organization methods employ the spontaneous
74 pattern formation capacity of cells to generate capillary network structures
75 (reviewed in [6]). Recent advances in the integrative studies of tissue engineering
76 and vascular biology have enabled construction of a perfusable vascular network
77 in vitro. For example, in 2013, a microfluidic device was developed with a self-
78 organized perfusable vascular network [14]. We have previously integrated a
79 spheroid culture system with the self-organized capillary network to improve the
80 culture conditions of spheroids [15,16].
81
82 Currently, these new culture methods are highly technical and difficult to
83 implement in a common biological laboratory. Various microfluidic chips are
84 commercially available [17], but collaboration with engineering researchers is
85 needed to obtain microfluidic devices with optimized designs. For perfusion itself,
86 syringe pumps are not very common in a biological laboratory, and it is still
87 technically difficult to connect tubes without collapsing the capillary network in a
88 gel.

In the present study, we developed an easy method to enable microcirculation in ordinary glass-bottom culture dishes. First, we screened commercially available endothelial cells for their capacity to form a lumen. Next, we developed a culture system to perfuse culture medium in the lumen. The flow persisted for 12–24 hours per one medium change, which enabled long-term perfusion. We observed the main features of the endothelial pattern formation, which correlated with flow, endothelial cell shape changes, collective migration towards the upstream of the flow, remodeling of the vascular network, extravasation of tumor cells, the effect of pericytes on pattern formation, and the perfusion of vascularized spheroids. These results show the usefulness of this culture method for elucidating various biological phenomena.

Materials and Methods

Cell culture

We used commercially available primary cultured cells to generate a perfusable vascular network based on a previous report [14]. The cells were human umbilical vein endothelial cells (HUVECs), human aorta endothelial cells (HAECs), human umbilical artery endothelial cells (HUAECs), human pulmonary artery endothelial cells (HPAECs), human microvasculature endothelial cells (HMVECs), and human lung fibroblasts (LFs) (Lonza Inc.). We used optimized growth media supplied by Lonza Inc. to maintain these cells. After screening for their pattern formation capability (Fig. S1), HUVECs were mainly used for experiments. We used LFs for the coculture system [18], which were maintained using FGM-2 culture medium and protocols provided by the manufacturer (Lonza Inc.). For visualization purposes, we used red fluorescent protein (RFP)-labeled HUVECs and GFP-labeled pericytes from Angio-proteomie Inc. HL60 and NMuMG-Fucci cells were provided by the Riken Bioresource Research Center (RCB2813 and RCB0041, respectively). Colon Tumor 26 (C26) is a colon cancer cell line isolated

from a BALB/c mouse treated with carcinogen *N*-nitroso-*N*-methylurethan [19]. C26 cells were injected into the spleen, and cells that metastasized to the liver were isolated. By repeating this injection-isolation cycle four times, LM4 cells were isolated. The details of LM4 cells will be described elsewhere (EK, manuscript in preparation). HL-60 and LM4-GFP cells were maintained in RPMI 1640 medium (Nacalai Tesque, Inc.) supplemented with 10% FBS and 1% penicillin-streptomycin.

Culture dishes

We developed a culture dish to exert static pressure on the self-organized capillary system. This dish consisted of standard 35- or 60-mm glass-bottom tissue culture dishes with a glass separator. The 12 phi glass well part was left open (Fig. 1a). This type of dish was obtained from a local manufacturer or assembled using a glass coverslip and bioinert adhesive such as replisil (silicone).

Generation of a self-organized vascular network

In the first protocol, endothelial cells generated a capillary network by self-organization and the culture medium was perfused into the network by static pressure. First, we mixed 1×10^7 HUVECs in a fibrin/collagen gel solution (5 mg/ml fibrin, 0.2 mg/ml type I collagen (rat tail, Enzo Life Sciences Inc., Alx-522-435-0020), and 0.15 U/ml aprotinin with a 1/150 volume of 0.5 U/ml thrombin). Then, we poured 150 µl of the fibrin/collagen/HUVEC solution into the well to separate the left and right halves of the dish divided by a glass separator. The dishes were incubated for 5 min at room temperature and then for 1 h at 37 °C to solidify the fibrin gel. Then, we added 5×10^5 LFs in a 5 mg/ml fibrin gel solution at the edge of a 35-mm culture dish to avoid physical contact of LFs and HUVECs. The dishes were incubated again for 1 h at 37 °C to solidify the fibrin gel. Then, we added 1 ml EGM-2 with 10 µM tranexamic acid to each well of the culture dish (total amount: 2 ml) and incubated the dish for 7 days (depending on the HUVEC activity, the culture period may be shorter). Culture media were changed once every 2–3 days. After confirmation of capillary network formation with lumens, we cut the edge of the preformed network using tungsten needles or a sharp

149 scalpel to make open ends. Then, we removed the culture medium from both wells
150 and added 1 ml of culture medium to one of the wells. The existence of flow was
151 confirmed by the flow of cell debris (Supplemental movie S2). Depending on the
152 flow resistance, the water level difference persisted for 24 hours.
153
154 Observation of vascular extravasation of neutrophils and tumor cells
155 Neutrophil-like differentiated HL-60 (dHL-60) cells were prepared by treating
156 HL-60 cells with 1.25% DMSO (Nacalai Tesque, Inc.) for 2 days. Two pieces of
157 thin PDMS sheet of roughly 6–8 mm in size were placed on the glass bottom in
158 parallel to each other and perpendicular to the glass separator before applying the
159 HUVEC-containing fibrin gel. HL-60 and dHL-60 cells were visualized with
160 CellTracker Green CMFDA (1:1000, Thermo Fisher Scientific). Then, 4×10^6
161 HL-60, 1×10^6 dHL-60, or 1×10^6 LM4-GFP cells were suspended in 2 mL
162 EGM-2 and applied to one side of the dish. For endothelial activation, 10 ng/mL
163 human recombinant TNF-α (PeproTech, Inc.) was added to the medium
164 overnight before the experiment. The HUVEC vascular network was visualized by

165 incubation with rhodamine-conjugated UEA-I lectin (1:1000, Vector
166 Laboratories) for 60 minutes in advance. Time-lapse and z-stack observations
167 were performed with a Nikon A1R microscope.
168
169 Generation of perfusable spheroids with vasculature
170 We also developed a protocol to perfuse spheroids with an endothelial cell
171 vasculature (Fig. 8a). First, we prepared spheroids containing target and
172 endothelial cells, and embedded the spheroid in a 2-well dish with fibrin gel. After
173 the spheroids sprouted, we cut the tip of the sprout with a sharp scalpel and
174 exerted static pressure for perfusion. Detail of the protocol is described below.
175
176 First, we prepared HUVECs, target cells, and lung fibroblasts. Then, we mixed
177 HUVECs, lung fibroblasts, and target cells in a Sumiron MS-9096U 96-well dish.
178 The ratio of HUVECs:LFs:target cells was 40:10:4. We cultivated the spheroids
179 for 2 days.
180

Next, we embedded spheroids in the culture dish. We prepared the culture dish, fibrin, and thrombin solution. The culture dish was cooled on ice. We collected the spheroids in a 1.5-ml Eppendorf tube and removed the supernatants. Next, we added 150 µl of the fibrin gel solution to the Eppendorf tube on ice. Then, we added 1 µl of the thrombin solution to the Eppendorf tube, quickly agitated the spheroids, and then transferred the solution to the 2-well dish. We moved the dish to the stage of an inverted microscope (×2 objective lens) and carefully adjusted the locations of the spheroids using tungsten needles. The fibrin gel was solidified for 5 min at room temperature and then for 1 hour at 37 °C. During this period, we prepared LFs mixed with the fibrin gel solution. Finally, we added the thrombin solution to the LF-fibrin solution and then transferred the LF-fibrin gel solution to the side of the 2-well dish. After the fibrin gel solidified for 1 hour at 37 °C, we added 2 ml EGM-2 with 10 µM tranexamic acid and incubated the dishes for 7 days for the sprouts to elongate. In some cases, we seeded HUVECs on the solidified fibrin gel to prevent leak. Culture media were changed once every 2–3 days.

197

198 ## Flow tracers

199 We used various flow and permeability tracers to observe the characteristics of
200 flow. Whole blood from a volunteer was diluted 10-fold with EGM-2 culture
201 medium to observe red blood cell perfusion of the capillary network. Fluorescent
202 particles (5 μm, Duke Scientific) were used to visualize flow for particle image
203 velocimetry (PIV). FITC-dextran (70 kDa) was used for the permeability
204 experiment. We also used diluted milk (1/1000) as a tracer for brightfield imaging.

205

206 ## Histology and immunohistochemistry

207 Cultured blood vessels and spheroids were fixed in 4% PFA
208 (immunohistochemistry) or Bouin's fixative (HE staining) overnight. Fixed
209 specimens were dehydrated using 70% ethanol in situ, detached from the culture
210 dish, and transferred to a glass bottle. The samples were further dehydrated in
211 graded concentrations of ethanol. Then, the ethanol was substituted with xylene
212 and paraffin. The paraffin block was cut at 10 μm thicknesses. For histology, these

213 sections were stained with hematoxylin and eosin.

214

215 For immunohistochemistry and Tdt nick end labeling (TUNEL), sections were
216 deparaffinized and stained using the protocols provided by the manufacturers.
217 Antibodies against PDGFB (Abcam, ab23914), type IV collagen (LSL, LB-0445),
218 and desmin (LabVision, MS-376-S0) were used. To detect apoptotic cells, we
219 used an In situ Apoptosis Detection Kit (Takara Bio, MK500).

220

221 Image acquisition and analysis

222 Observation of three-dimensional structures was conducted using a Nikon A1R
223 confocal microscope. For long-term observation of the whole culture dish, we used
224 a Keyence BZ-900 with a tiling function. All image analysis was performed using
225 ImageJ [20] or Fiji [21]. To observe vessel wall movement in long-term culture,
226 we used the “linear stack alignment with SIFT” plugin for registration of the
227 figures obtained at various time points. We used the “Reslice” command to
228 prepare kymographs of cell movements from time-lapse movies.

Results

Pattern formation capability of commercially available primary cells

First, we screened commercially available human endothelial cells for their pattern formation capacity. The tested cells were HUVECs, HAECs, HMVECs, and HPAECs (Fig. S1). These cells were cultivated in normal glass-bottom dishes, Matrigel, collagen gel, and fibrin gel. In principle, all tested primary cell cultures were capable of generating a network of perfusable lumens only when the cells were cultivated in fibrin gel with human LFs, indicating that we could choose any type of primary endothelial cell. One exception was HPAECs that generated a perfusable network in fibrin gel without lung fibroblasts. This characteristic was observed in cells with low passage numbers up to 3.

Method for culture medium perfusion

Next, we developed a culture method to perfuse the self-organized network in a glass-bottom dish. Using the protocol described in the Materials & Methods, we induced flow in the self-organized capillary network. First, we prepared a glass-

246 bottom dish separated by a glass separator (Fig. 1a). Next, we allowed the cells to
247 self-organize and generate a vascular network with a lumen in a gel that separated
248 two wells of the dish. A mixture of HUVECs and fibrin gel was placed in the well
249 of the glass-bottom dish (Fig. 1b) and allowed to solidify for 30 min. Lung
250 fibroblasts for coculture were mixed in fibrin gels and placed at the edge of the
251 culture dish to avoid contamination of lung fibroblasts in endothelial cell networks
252 because fibroblasts inhibited formation of the endothelial cell network by direct
253 contact (Fig. 1c). Finally, the culture medium was added, and the cells were
254 incubated in a CO_2 chamber (Fig. 1d).
255
256 After 1 week, the vascular network with a lumen was generated spontaneously (Fig.
257 1e, g). Next, we exerted static pressure on the preformed capillary network as
258 follows. First, we made a cut to generate open ends of the capillary network (Fig.
259 1e. h). Then, we removed the culture medium from both wells and added culture
260 medium (and tracer) to one of the wells (Fig. 1f, i). If the lumens were connected,
261 we observed flow using the various tracers. We perfused fluorescent beads to

detect the perfusability of the capillary network (Fig. 1j, Supplemental movie S1). However, the fluorescent beads adhered to the endothelial cell surfaces and interfered with the fluorescence observation. Therefore, this method was used only once per experiment. When whole blood diluted with EGM-2 was loaded, we observed the flow of red blood cells in the self-organized capillary network (Fig. 1k, l, Supplemental movie S2).

Formation of a lumen around a solid object

In this culture system, lumen formation only occurred near the periphery of the culture well. Thick, perfusable lumens were formed in the region at 1 mm around the culture well wall or separating glass plate. This was not due to the high cell density around the periphery of the dish because increased cell density did not induce lumen formation in the center of the dish (Fig. S2a–d). We induced lumen formation by embedding hard objects in the gel. When we mixed glass beads (1 mm diameter) with HUVECs at the beginning of the culture and cultivated the cells for 120 hours, we observed lumen formation around the glass beads (Fig.

278 S2e–h).

279

280 Flow-induced collective cell migration and cell shape changes in the culture system

281 In this system, we observed the dynamics of endothelial cells in response to flow
282 (Fig. 2). It is known that, at a certain range of flow rate, endothelial cells migrate
283 collectively toward the upstream of blood flow[22–24]. We easily observed this
284 phenomenon in our culture system. We used Hoechst 33342 as a vital stain of
285 endothelial cell nuclei and exerted flow to a 35-mm culture dish. We then observed
286 the collective upstream movement of endothelial cells (Fig. 2a–c). In the region
287 with flow, the cells migrated collectively upstream of the flow (Fig. 2b). The white
288 arrow indicates the orbit of cell debris, indicating that the direction of cell
289 movement was opposite to that of the flow. In contrast, only random movement
290 of cells was observed in the non-flow region (Fig. 2c), indicating that this system
291 is useful to assess flow-endothelial cell interactions.

292

293 We next observed endothelial cell shape changes induced by the flow. In the fast

294 flow region, endothelial cells became elongated parallel to the direction of flow
295 (Fig. 2d–g). In the slow flow region, the endothelial cells remained unpolarized
296 (Fig. 2h–k). In the non-flow region, the endothelial cells formed isolated cysts with
297 cell debris inside (Fig. 2l–n).
298
299 Reconstruction of vascular remodeling by long-term flow in the vasculogenesis
300 system
301 Because flow could be slow depending on the geometry of vasculature and the size
302 of the cut, we maintained the flow for a long time. As the reservoir medium
303 decreased, the pressure gradient changed. In general, we could maintain flow for
304 24 hours, which allowed long-term flow effects. We confirmed the flow by
305 observing the flow of cell debris in the brightfield view (Supplemental movie S3).
306 Unlike a two-dimensional culture system, HUVECs could be maintained for a very
307 long period of up to 1 month without degradation of the fibrin gel (Fig. 3a–c). The
308 openings remained unobstructed after 4 weeks of culture (Fig. S3). A high
309 magnification view revealed the occurrence of the remodeling process (Fig. 3d, e).

In the region with flow, the radius of the vascular segment was increased gradually (Fig. 3d, d', Supplemental movie S4). In the region without flow, the vasculature was degraded gradually and finally became fragmented vascular cysts (Fig. 3e, e', Supplemental movie S5).

Histological observation confirmed the remodeling process in this culture system. The top of the culture area was covered with HUVECs (Fig. 3f, g). The flow region was covered by a relatively thick HUVEC sheet (Fig. 3f, h). The non-flow region contained several apoptotic bodies (Fig. 3f, i). To confirm the distribution of cell death, we applied TUNEL staining. Positive signal was observed in the non-flow region (Fig. 3j, k), confirming the histological observation. We also observed an extracellular matrix sheath in which the basement membrane remained, while endothelial cells were retracted in the non-flow region (Fig. 3l). These observations supported that vascular remodeling occurred in this culture system.

Effect of vascular flow on cell proliferation

326 Because the physiological role of vascular flow is the transfer of oxygen and
327 nutrients, we examined the effect of flow on cell proliferation outside the blood
328 vessel. We used Fucci-containing NMuMG cells, with which we could dynamically
329 observe the cell cycle, to easily assess the effect of oxygen-nutrient transport by
330 the flow on the mesenchyme region. NMuMG cells were mixed with RFP-HUVEC
331 suspensions and cultivated for 1 week. The NMuMG cells formed sparse colonies
332 in the region away from the vasculature, and the vasculature became narrower,
333 presumably due to the competition between HUVECs and NMuMG cells (Fig.
334 4a). Next, we made a cut to only a part of the network to form flow and non-flow
335 regions (Fig. 4b). We then compared the number of proliferating cells in flow and
336 non-flow regions and detected increased fluorescence by exerting flow for 2 days
337 (Fig. 4c–e), indicating that the medium flow was effective for tissue maintenance
338 in this culture system.
339
340 Dynamics of pericytes in the self-organized vascular network
341 Pericytes reside around endothelial cells and modulate their biological functions

342 [9]. It has been reported that pericytes play an important role in the vascular
343 remodeling process to generate a hierarchical vascular tree structure in developing
344 retina [25]. To examine whether addition of pericytes to this culture system
345 affected the remodeling process, we cocultured pericytes in this culture system
346 and observed the long-term pattern change with flow. Vasculature with pericytes
347 grew normally, and we maintained the culture system with pericytes for up to 1
348 month (Fig. S4a, b). After 1 month, the vasculature was still perfusable without
349 leak (Fig. S4c, d). The morphology of vasculatures with pericytes was similar to
350 that without pericytes (Fig. S4c, d). In the region with flow, the diameter of the
351 vascular segment was increased (Fig. S4e, e'), whereas in the region without flow,
352 the vasculature was degraded gradually (Fig. S4f, f'). Unfortunately, the final
353 shape of the vascular network with pericytes appeared more or less the same
354 compared to that without pericytes (Fig. S4a–d).
355
356 Interestingly, pericytes disappeared around the fast flow region and surrounded
357 the endothelial vasculature in the non-flow region (Fig. 5a, b). Initially, pericytes

were distributed evenly (Fig. 5a). After 3 weeks of culture, spots of high pericyte cell density appeared in non-flow regions (Fig. 5b, arrows). However, in the fast flow region, the pericytes had disappeared (Fig. 5b, red circle). We observed active migration away from the fast flow region (Fig. 5c. d, Supplemental movie S6). In the fast flow region, a very small number of pericytes was observed (Fig. 5e). At the interface between flow and non-flow regions, we observed an increase of pericytes only in the non-flow region (Fig. 5f). In the non-flow region, we observed pericytes wrapped around cysts of endothelial cells containing debris (Fig. 5g). To understand the reason for this uneven distribution, we observed the distribution of PDGFB, a chemoattractant for pericytes (Fig. 5h–k). In the flow region, the PDGF signal was low, while in the non-flow region, strong signals were detected in endothelial cell cysts and pericytes (Fig. 5h–k). This result suggested induction of PDGFB in the non-flow region was one of the reasons why pericytes only remained in the non-flow region.

374 Reproducing extravasation of inflammatory cells from the capillary network

375 We next observed the interaction of blood cells and capillaries using this synthetic
376 system. At first, we perfused fluorescent beads (Fig. 1j) or red blood cells (Fig.
377 1k–l) in the self-organized vascular network. We also perfused the neutrophil cell
378 line HL-60 in the self-organized vascular network (Fig. 6a, b, Supplemental movie
379 S). We differentiated HL-60 cells by DMSO treatment and perfused the cell
380 suspension in the self-organized vascular network. The cells had the ability to
381 move through a very thin capillary segment (Fig. 6c). We also observed the time
382 course of extravasation (Fig. 6d–f). Three-dimensional observation confirmed
383 that the HL-60 cells were outside of the vascular network (Fig. 6g).

384

385 Reproducing metastasis of cancer cells from capillary vessels

386 The other possible application of this culture system is assessment of
387 hematogenous metastasis. We introduced the cancer cell line LM-4 into the
388 culture medium with perfusion and observed the dynamics for up to 48 hours. As
389 a result, the cells flowed inside the self-organized vascular network (Fig. 7a). The

390 cells also changed their shape during emigration from the vascular lumen (Fig.
391 7b). We next observed the detailed morphology of cancer cells after extravasation.
392 The emigrated cells maintained adherence to the vascular wall after extravasation
393 and extended protrusions along the endothelial cell surface (Fig. 7c-c''), which
394 may be regarded as filopodia-like protrusions in hematogenous metastasis [26].
395 In some cases, the extravasated cells influenced the shape of the vasculature (Fig.
396 7d, d'). We also observed vascular wall retraction at the sight of the extravasated
397 cancer cells.
398
399 Vascularized spheroid culture system with flow
400 We reproduced the spheroid culture system with perfusable vasculature [15] with
401 a slight modification of the protocol (Fig. 8a). First, we produced spheroids using
402 a 96-well plate. Then, the spheroids were embedded in the fibrin gel underneath
403 a glass separator. When we cultured the spheroids for 1 week, HUVECs formed
404 sprouts with a lumen, which were as long as 1 mm (Fig. S5). Then, we cut the tip
405 of the sprouts to perfuse culture medium inside the vascular lumen.

406

407 By exerting static pressure between two wells, we observed the medium flow in

408 the connected spheroids (Fig. 8b). Interestingly, if we set two spheroids in close

409 vicinity, the vascular sprouts from both spheroids fused and made a serial cluster

410 of spheroids with perfusable vasculature.

411

412 ## Discussion

413 ### Reconstructive system of pattern formation

414 In the present study, we constructed a simple perfusion system to reproduce the
415 flow in a capillary network. The seminal work on this type of culture system with
416 flow was performed by Noo-Li Jeon's group [14]. However, the system needs an
417 elaborate microfluidic device that can only be fabricated by researchers with
418 access to clean room facilities, and it is time consuming for biologists to fully use
419 the system including the device, tubing, and syringe pump. In contrast, our system
420 employs a standard glass-bottom dish without any additional pump, tubing,
421 reservoir, or engineering. The simplicity of the system enabled us to combine it
422 with time-lapse observation on a stage top incubator without any additional
423 apparatus. However, there are several shortcomings because of its simplicity. For
424 example, we could not regulate the flow rate in this system accurately because the
425 driving force for perfusion is static pressure between two wells. For detailed
426 control of flow, we need to use microfluidic devices.

427

Lumen formation capability of endothelial cells

The mechanism of lumen formation by endothelial cells remains to be elucidated. ECM degradation and apicobasal polarity formation are thought to play a role [27]. In our culture system, one factor was the diffusible signaling molecules from LFs. HUVECs cultivated in fibrin gel formed a network even without LFs, but we could not induce a lumen without coculture with LFs. Two reports used a proteomics approach to identify the diffusible factor responsible for lumen induction by LFs. They identified several factors, but the effect of the combination of these factors was less effective than lung fibroblast coculture [28,29]. We also found that lumens were preferentially formed at regions near a hard object (Fig. S2). One possible mechanism may be high cell density due to preferential migration of cells toward the hard substrate (durotaxis) [30], but increasing the cell density as a whole did not increase the lumen formation region around hard objects. In addition, the lumen formation capacity of HUVECs and LFs differed significantly depending on the production batch. We sometimes experienced HUVECs and LFs whose proliferation appeared to be normal, but lumen formation was poor.

444 Increasing cell numbers sometimes compensated for the low lumen formation
445 activity, but in many cases, using a different batch of cells improved lumen
446 formation.
447
448 Effect of the extracellular matrix on the pattern formation mechanism
449 We used fibrin gel to generate a perfusable vascular network based on a previous
450 study [14]. Fibrin is the main component of a blood clot and not used in
451 physiological tissues. We tried to substitute fibrin gel with other physiological
452 extracellular matrixes such as Matrigel and type I collagen without success. This
453 may be due to the physical viscosity difference. A fibrin gel solution is less viscous
454 than a collagen gel solution. As a result, suspended HUVECs in fibrin gel gathered
455 at the bottom of a dish because of gravity. We succeeded in generating a lumen
456 structure in a type I collagen gel by embedding HUVEC spheroids, indicating that
457 the local cell density may be critically important.
458
459 Dynamics of pericytes in the capillary network with flow

For recruitment of pericytes to nascent blood vessels, platelet-derived growth factor B (PDGF-B) produced by tip endothelial cells plays pivotal roles [25,31]. Notably, tip endothelial cells adjacent to hypoxic tissues are exposed to high concentrations of VEGF-A [31]. Moreover, because of the absence of lumens, tip endothelial cells have limited access to circulating blood [31]. Consistently, cultured HUVECs under high oxygen pressure exhibit reduced production of PDGF-B [32]. In our pericyte-HUVEC coculture with flow, pericytes unexpectedly disappeared in the flow region. A possible reason may be the lack of PDGF-B in the flow region. Endothelial cells in the flow region were under normoxic conditions. There are no flow regions in which endothelial cells should produce PDGF-B [32], and because of the PDGF-B gradient, pericytes might migrate away from the flow region or extensively proliferate at non-flow regions.

Connection of two vasculature systems

The connection between two different capillary systems still remains a major challenge. We tried to establish connections between the self-organized HUVEC

476 vascular network and the vascular network in embryonic tissue. The endothelial
477 cells from the embryonic tissue appeared to adhere to the HUVEC structure.
478 However, the lumens of these vasculatures did not form a connection. Therefore,
479 we could not perfuse the vasculature in embryonic tissue (Fig. S6). Additional
480 factors may be necessary to use this culture system as an alternative to organ
481 culture. Because direct connection of two vascular systems is still a major
482 challenge, currently, a technically simpler experimental model of vasculature-
483 blood cell interactions may be a major field of application. In the present study,
484 we demonstrated two applications, dynamics of inflammatory cells and
485 hematogenic metastasis. Various other system can be implemented with our
486 current model without additional costs.
487
488 Relationship between microfluidic device methods
489 This method may be a very good prescreening method for microfluidic device
490 experiments. The major merit of this method is the ease and low cost. We have
491 experienced difficulty in introducing blood vessel into a microfluidic device [15]

because it requires specialized skills to connect tubes without damaging gels or endothelial cell networks. As a result, it is difficult to perform a large number of microfluidic device experiments because of its technical difficulty. Although we only used a constant pressure condition for medium perfusion and could not strictly control the flow, this method may be a good starting point to roughly estimate the effect of flow in biological laboratories.

Acknowledgments

The authors thank Professor Fumio Arai for helpful suggestions. We also thank Mitchell Arico from Edanz Group (https://en-author-services.edanzgroup.com/) for editing a draft of this manuscript. This work was financially supported by JST CREST (Grant Number JPMJCR14W4).

Author contributions

Kei Sugihara, Yoshimi Yamaguchi, and Shiori Usui undertook experiments. Yuji

508 Nashimoto and Sanshiro Hanada provided materials and designed experiments.
509 Etsuko Kiyokawa provided tumor cell lines. Akiyoshi Uemura designed
510 experiments, provided materials, and wrote the pericyte-related section in the
511 manuscript. Ryuji Yokokawa, Koichi Nishiyama, and Takashi Miura designed
512 experiments and wrote the manuscript.
513

514 Figure Legends

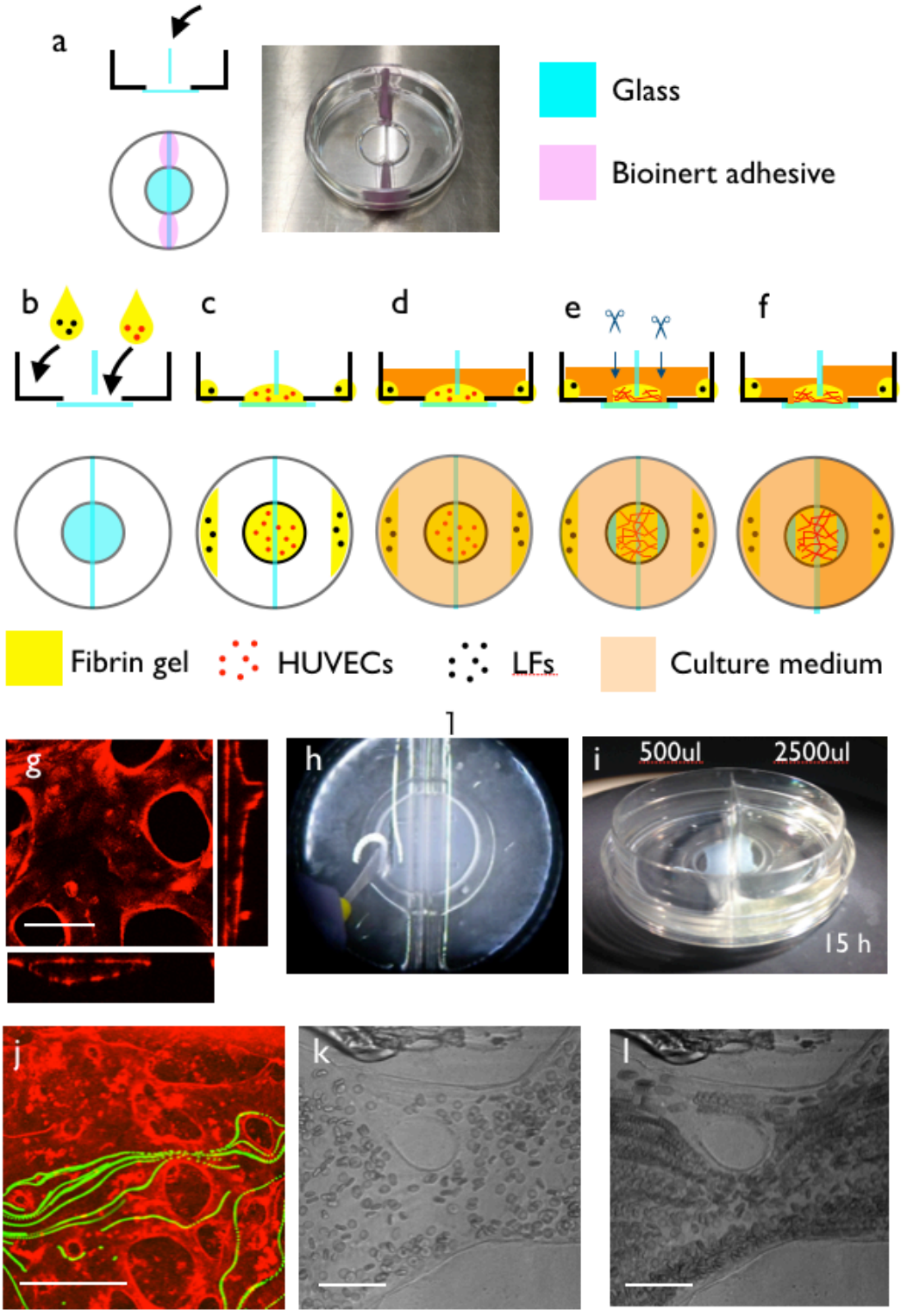

515

Figure 1: Culture system setup. (a) Side and top views of the culture dish before setup. The dish was a normal 12-phi glass-bottom dish. A glass separator was set at the center of the dish with a bioinert adhesive. (b) First, we placed 150 µl fibrin gel mixed with HUVECs in the center of the glass plate, so that two sides of the dish were separated by the glass separator and fibrin gel. We also added LF-containing fibrin gel at the edge of the dish. (c) We incubated the dish for 30 min to solidify the fibrin gel. (d) We added 1 ml culture medium to both wells and incubated the dish for 1 week. (e) After 1 week of culture, a vascular network with a perfusable lumen was formed in the glass-bottom region. Then, we cut both edges of the regions to make openings. (f) After the cuts, we increased the amount of culture medium on one side of the dish. This caused a static pressure difference between both openings of the self-organized capillary network, resulting in steady flow inside the apparatus. (g) A vascular network with a lumen was generated in the fibrin gel region. RFP-HUVECs were cultivated in the fibrin gel, and we observed the vascular network with lumens. (h) After the vascular network was formed spontaneously, both sides of the network were cut to make openings. (i)

532 After making the cuts, we moved the culture medium, so we could exert static
533 pressure to one side of the vascular network. The water level difference was
534 maintained overnight, depending on the degree of lumen formation in the
535 vascular network). (j) Flow inside the lumen was visualized using fluorescent
536 beads. (k) Snapshot of the culture system when using whole blood as a tracer. Red
537 blood cells were flowing inside the self-organized vasculature. (l) Projection of
538 multiple frames of (k). Movements of red blood cells were visualized as a stream.
539 Scale bars: 100 μm (g); 500 μm (j); 50 μm (k, l).
540

541

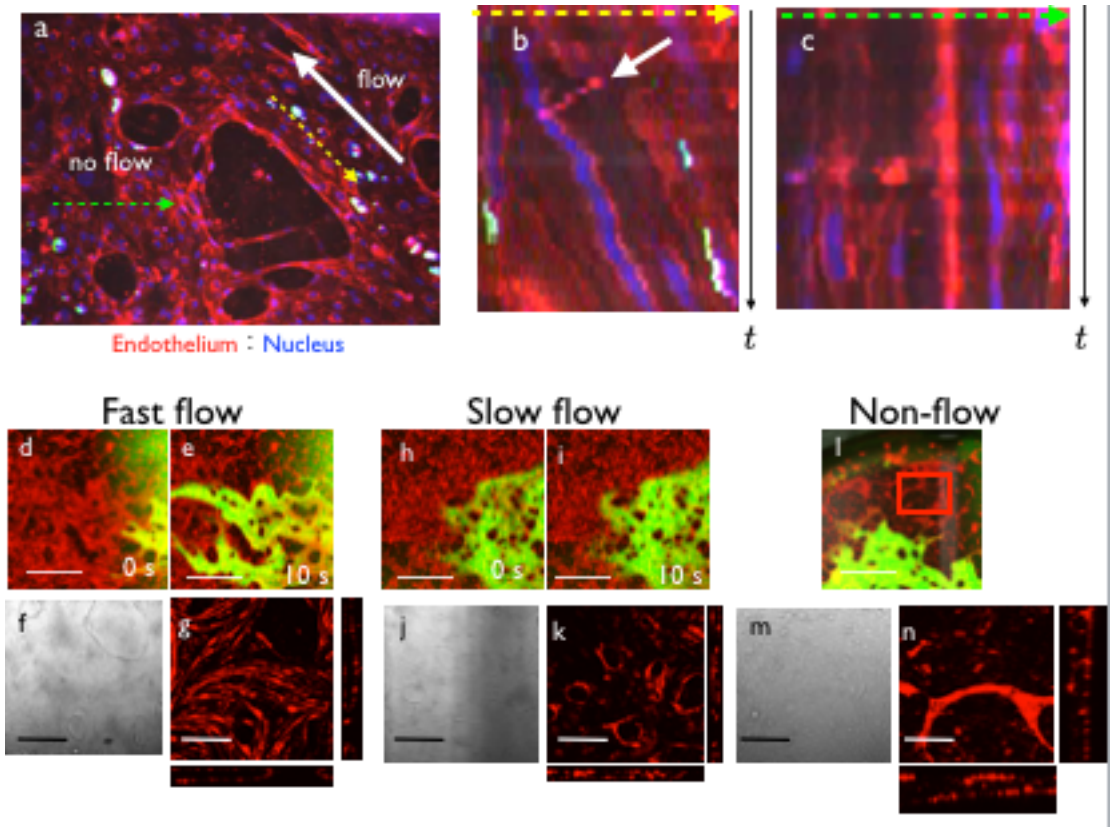

542

543 Figure 2: Flow-induced collective cell migration and cell shape changes. (a) Initial

544 shape of the vascular network. HUVECs were stained with UEA1 and nuclei were

545 stained with Hoechst 33342. There was a flow-positive region (yellow-dashed

546 line) and non-flow region (green-dashed line). Direction of flow is indicated by a

547 white allow. (b) Kymograph of the yellow-dashed line region. Collective

548 movement toward upstream of the flow was observed. White arrow indicates the

549 flow of cell debris. (c) Kymograph of the green-dashed line region. Cell movement

was random. (d–n) Cell shape changes induced by flow: (d, e) Fast flow. When FITC dextran was perfused, the vessel regions near the inlet or outlet showed fast flow. (f) Brightfield view of the fast flow region. Endothelial cells became shaped as spindles aligned parallel to the flow direction. (g) Fluorescence view of the fast flow region. At the floor of the lumen, we observed spindle-shaped cells parallel to the flow direction. (h, i) Slow flow. When FITC dextran was perfused, the vessel regions far from the inlet or outlet showed slow flow. (j) Brightfield view and (k) confocal view of the slow flow region. Endothelial cells did not show any polarity. (l) Low magnification view of the non-flow region. (m) Brightfield view and (n) confocal view of the non-flow region. Vasculatures were disconnected and became thin endothelial cysts with cell debris inside. Scale bars: 1 mm (d, e, h, i, l); 200 μm (f, g, j, k, m, n).

563

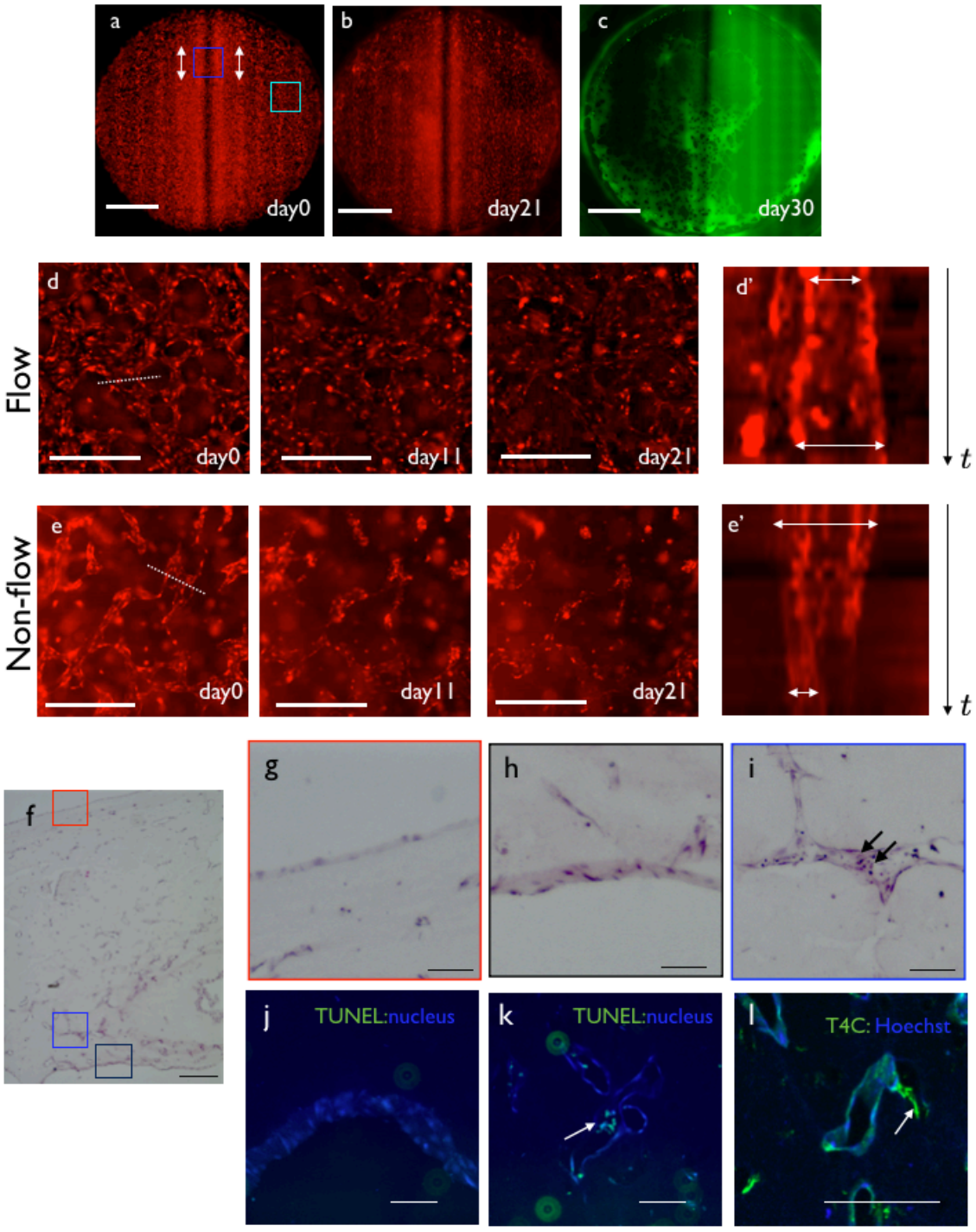

564

565 Figure 3: Reconstruction of flow-induced remodeling. (a–c). Time course of the
566 vascular network of the two-well dish. (a) Vascular pattern at day 0. Locations of
567 the cut (white arrows) and high flow region (blue box), non-flow region (cyan
568 box) are indicated. A cut was made at the periphery of the culture area to induce
569 regions of flow and non-flow within a single dish. (b) Vascular pattern at day 21.
570 (c) Visualization of the perfusable area by FITC-dextran. Perfusable regions
571 existed near the inlet and outlet, near the glass separator and edge of the well. (d).
572 Remodeling process at the high flow region from day 0 to 21. (d') Kymograph of
573 the dotted line region in (d). Vasculature dilated gradually. (e) Remodeling
574 process at the non-flow region from day 0 to 21. (e') Kymograph of the dotted line
575 region in (e). The vascular diameter decreased. (f) Low magnification view of a
576 hematoxylin-eosin-stained EC monoculture sample. (g) Magnified view of the
577 upper surface of the gel. The surface of the gel was covered by endothelial cells.
578 (h) Magnified view of the large lumen inside the gel. The lumen was also covered
579 by endothelial cells. (i) Magnified view of the small lumen inside the gel. Small
580 necrotic cells were observed inside the lumen (arrows). (j) TUNEL staining of the

581 flow region. No dead cells were observed. (k) TUNEL staining of the non-flow
582 region. Dead cells were observed inside the vasculature. (l) Type IV collagen
583 staining of the long-term culture sample. There were some lumens positive for
584 type IV collagen without cells (arrows), indicating the ECM sheath of the
585 degraded vasculatures in non-flow regions. Scale bars: 3 mm (a–c); 500 μm (d–f);
586 100 μm (g–l).
587

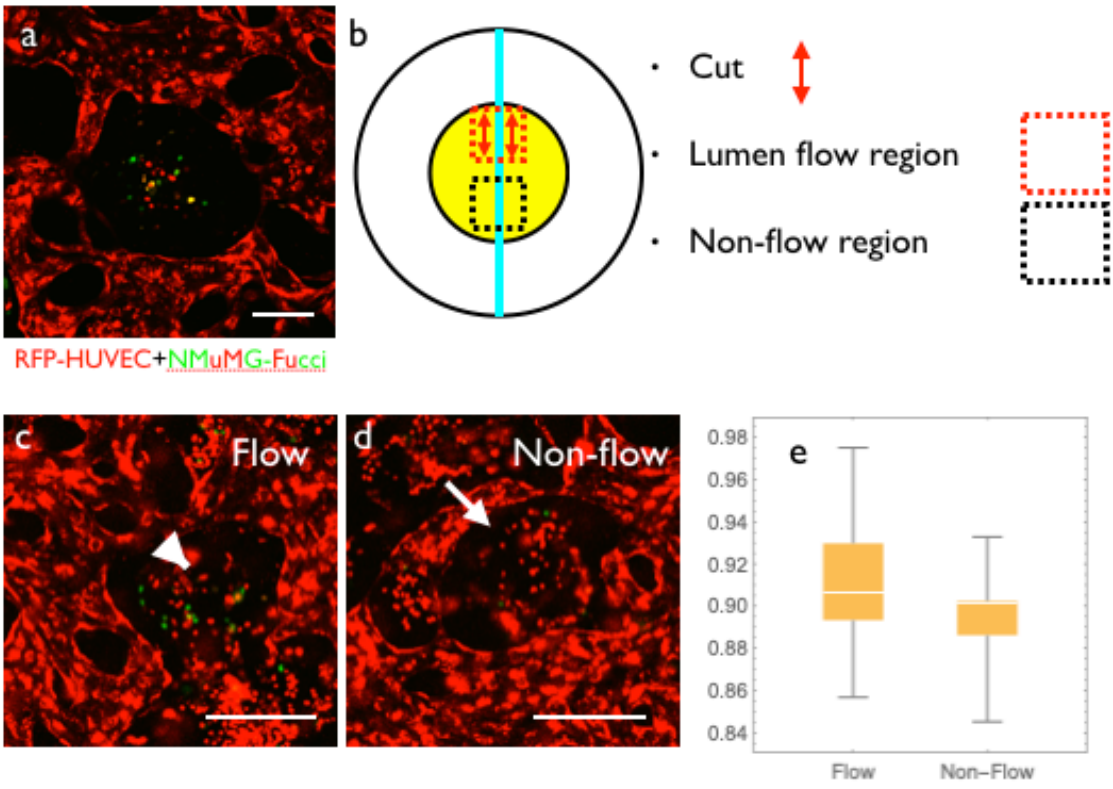

588

589 Figure 4: Effect of flow on cell proliferation. (a) Coculture of RFP-HUVECs and

590 NMuMG-Fucci cells. HUVECs and NMuMG cells segregated, and NMuMG cells

591 formed a colony in the interstitial region. (b) Experimental design. The upper

592 region (red-dotted line) was cut to induce flow inside the lumen. We did not

593 observe flow in the lower region (black-dotted line). (c) Flow region at 48 h.

594 Proliferative cells remained in the interstitial region (white arrowheads). (d) Non-

595 flow region at 48 h. Proliferating cells disappeared in the interstitial region (white

596 arrows). (e) Relative green fluorescence intensity ratio (24 h/0 h). A statistically

597 significant difference was found between flow and non-flow regions (Mann-

598 Whitney test, $p<0.05$). Scale bars: 200 μm.

599

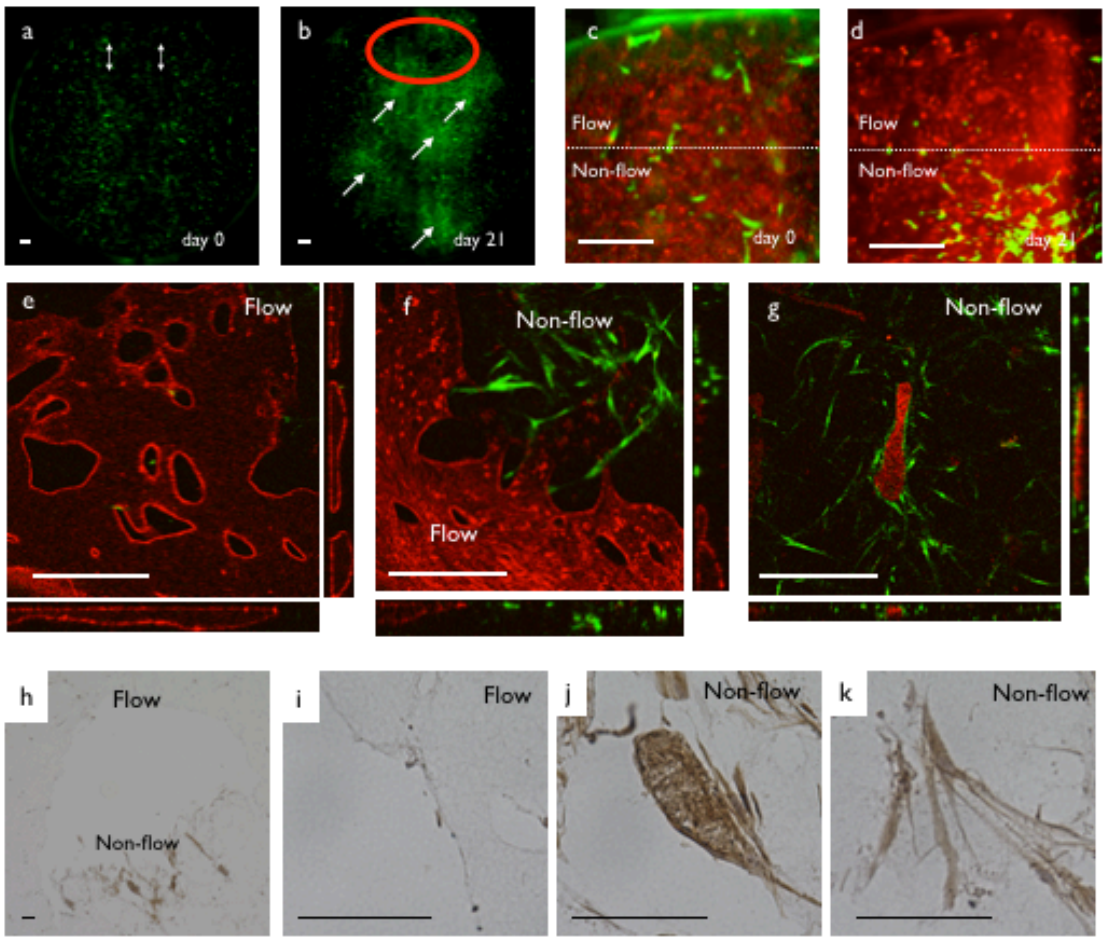

600

601 Figure 5: Dynamics of pericytes in the HUVEC-pericyte coculture system. (a)

602 Low magnification view of the distribution of pericytes at day 0 (green). White

603 arrows indicate the inlet and outlet. (b) Distribution of pericytes after 21 days of

604 perfusion culture. We observed a high density region of pericytes (arrows) in the

605 non-flow region and a low density region (red circle) in the flow region. (c) High

606 magnification view of pericyte distribution at the flow region (day 0). (d) High

607 magnification view of the pericyte distribution at the flow region (day 21).

608 Pericyte cell density was decreased in flow region and increased in non-flow
609 region. (e) 3D structure of the flow region at day 30. Endothelial cells (red)
610 formed vasculature with a perfusable lumen. Pericytes were virtually absent. (f)
611 Boundary between flow and non-flow regions. Pericytes resided in the non-flow
612 region. (g) 3D structure of the non-flow region. Vasculature was degraded and
613 flat cysts of endothelial cells with cell debris inside remained. Pericytes appeared
614 to surround the degraded structure. (h) Low magnification view of PDGFBB
615 immunohistochemistry. A positive signal was observed in the non-flow region. (i)
616 High magnification view of the flow region. No positive signal was observed. (j)
617 High magnification view of the non-flow region. The cell cyst and surrounding
618 pericytes had a high staining intensity. (k) High magnification view of pericytes
619 in the non-flow region. A positive signal was observed in the cytoplasm. Scale bars:
620 500 μm (a–g); 100 μm (h–k).
621
622

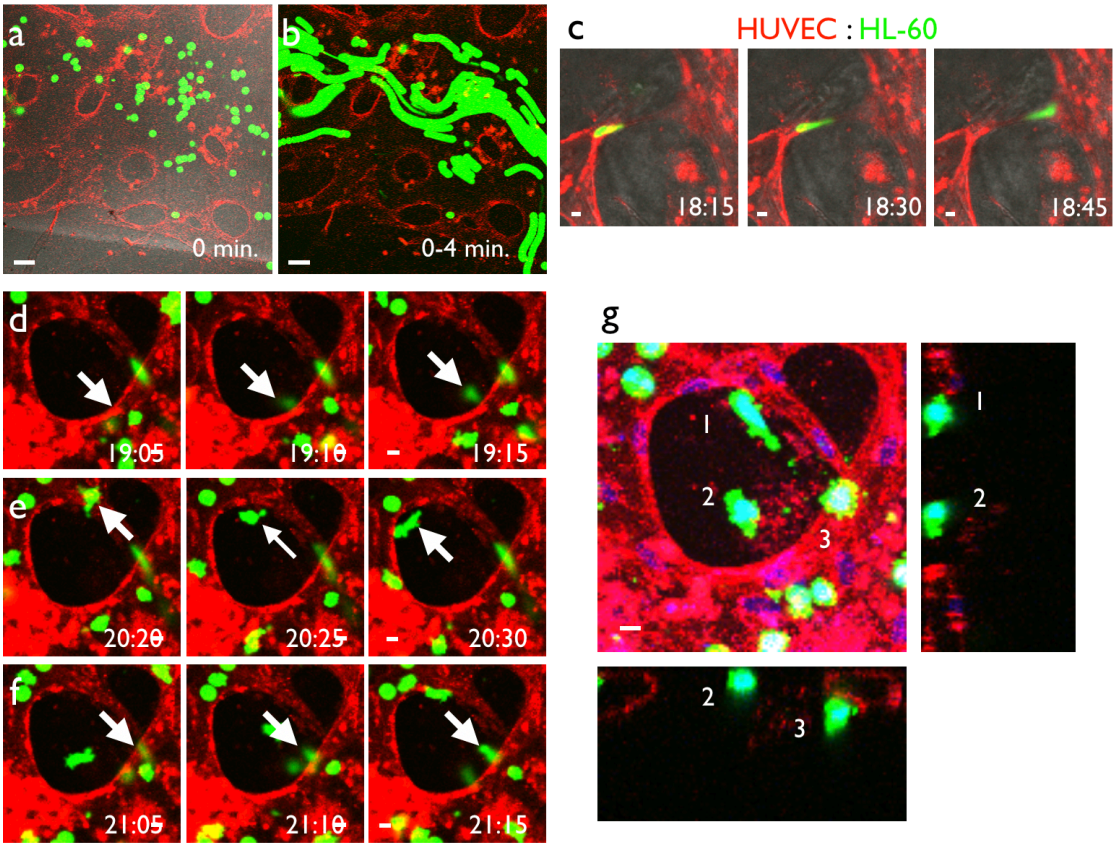

623

624 Figure 6: Extravasation of leukocytes using the self-organized vascular network.

625 (a) HL-60 cells, an acute myelogenous leukemia cell line, were labeled with

626 CellTracker Green and introduced into the self-organized vascular system

627 visualized by UEA-I lectin. (b) Projection image of a time-lapse movie for 4

628 seconds. Movement of HL-60 cells inside the vascular network was observed. (c)

629 DMSO-induced differentiated HL-60 cells (dHL-60), which mimicked

630 neutrophils, passed through thin vessels with large deformation under the

631 presence of TNF α. (d–f) Representative time-course of extravasation.

632 Extravasation occurred within a short time period (10 min.). Extravasating cells
633 (white arrows) extended protrusions toward the outside of the blood vessel when
634 emigrating from the blood vessel lumen. (g) Three-dimensional structure of
635 extravasated cells (white arrows) shown as max projection x-y and x-z/y-z single
636 slice images. We clearly observed extravasated cells outside of the vasculature.
637 Time separated with colons indicates hours and minutes. Scale bars: 50 μm (a, b);
638 10 μm (c–g).
639

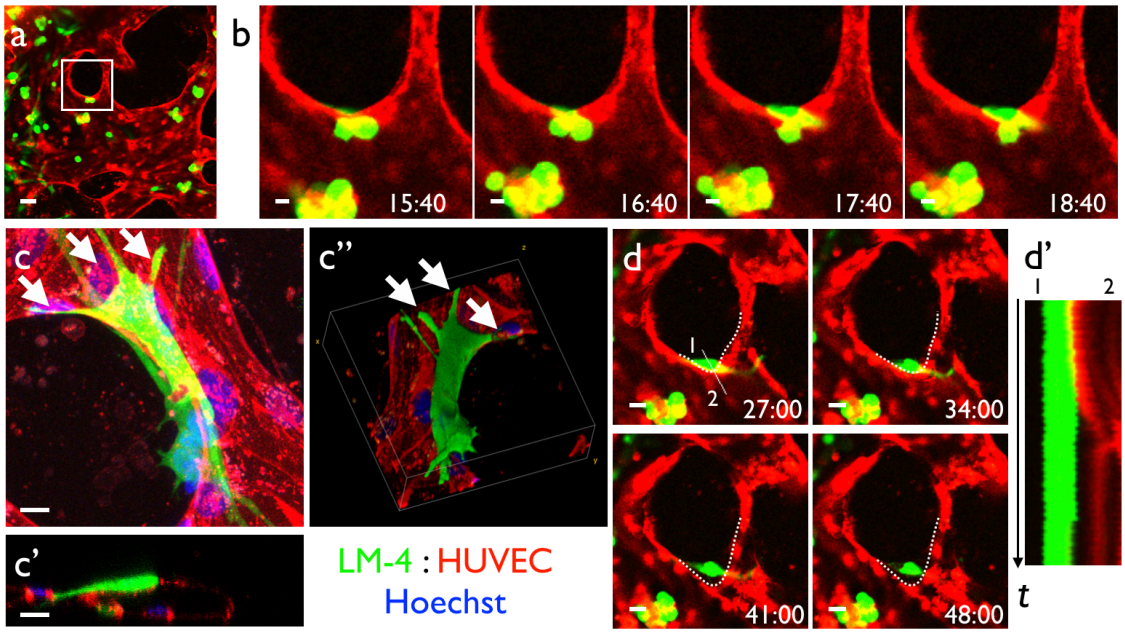

640

641 Figure 7: Reproduction of hematogenous metastasis of cancer cells from the

642 capillary network. (a) LM4-GFP cells were introduced into the self-organized

643 capillary network consisting of HUVECs visualized by UEA-1 lectin. (b) High

644 magnification time-lapse view of (a). We observed cancer cells emigrating out of

645 the blood vessels. (c) Detailed morphology of cancer cells on the endothelial cells.

646 Emigrated LM4 cells attached to the blood vessel with highly polarized

647 morphology and multiple protrusions. (c) Max projection image, (c') orthogonal

648 section, and (c'') 3D-reconstructed image. White arrows: cancer cell protrusions.

649 (d) Blood vessel shape changes after cancer cell emigration (white-dotted line).

650 (d') Kymograph of the blood vessel wall corresponding to the white line in (d).

651 Time separated with colons indicates hours and minutes. Scale bars: 50 μm (a);

652 10 μm (b, c); 20 μm (d).

653

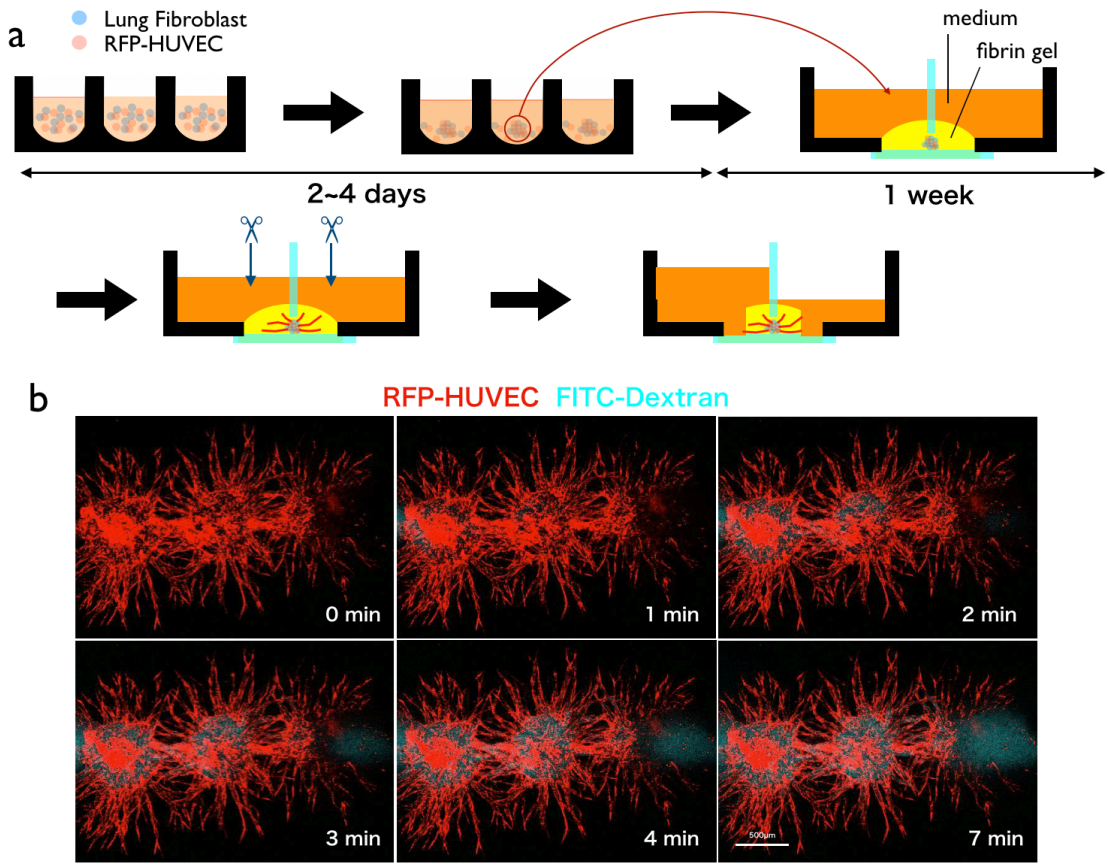

Figure 8: Perfusion of vascularized spheroids. (a) Experimental procedure. Spheroids containing RFP-HUVECs and lung fibroblast were generated and embedded in fibrin gel. After 1 week, sprouts from the spheroids became sufficiently long. Then, we cut the tip of the sprouts from both sides of the well and exerted static pressure to one side of the well. (b) Visualization of the perfusion inside the spheroid using FITC-dextran. Scale bar: 500 μm.

661 Supporting information

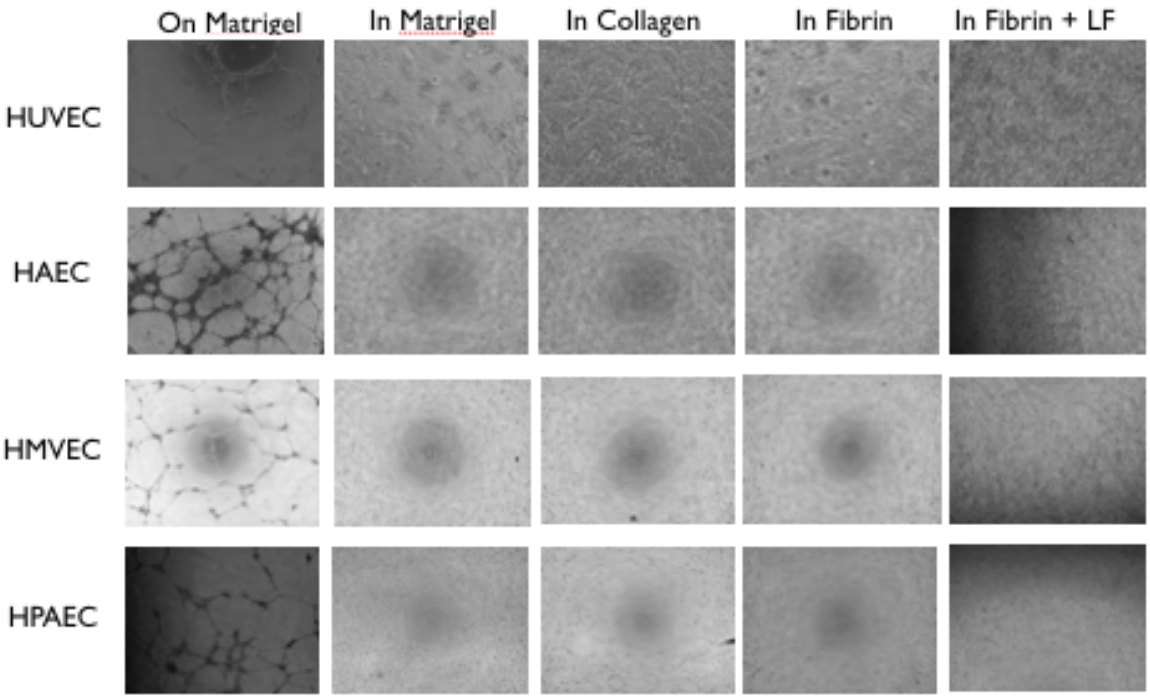

662

663 S1 Fig: Screening for the pattern formation capability of various commercially

664 available primary endothelial cells. All cells generated a meshwork structure on

665 Matrigel (tube formation assay). In Matrigel or collagen gels, the cells simply

666 became static and no pattern formation phenomena was observed. In fibrin gel,

667 the cells tended to connect to each other, but a lumen was not formed, except for

668 HPAECs. If we cocultured these cells with human lung fibroblasts (LFs), the cells

669 formed a network with lumens.

670

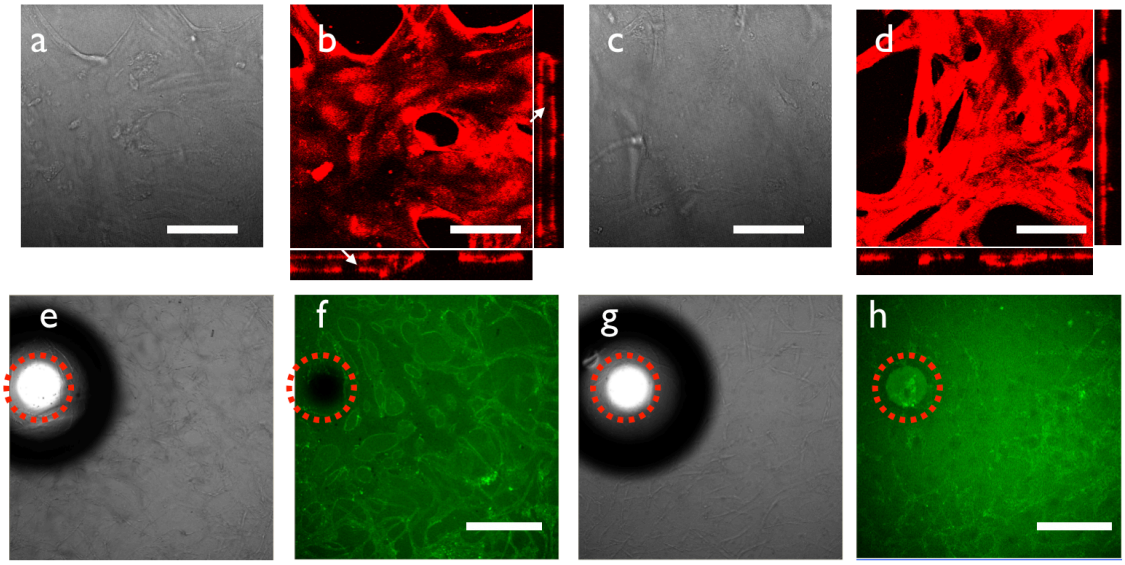

671

672 S2 Fig: Lumen formation was observed only around solid objects. (a) Brightfield

673 image of HUVECs cocultured with LFs in fibrin gel in the *periphery* of the dish.

674 A lumen structure was observed. (b) Fluorescence image of HUVECs cocultured

675 with LFs in fibrin gel in the *periphery* of the dish. HUVECs were stained with

676 UEA1-FITC. A lumen structure was observed (white arrows). (c) Brightfield

677 image of HUVECs cocultured with LFs in fibrin gel in the *center* of the dish. A

678 lumen structure was not clear. (d) Fluorescence image of HUVECs cocultured

679 with LFs in fibrin gel in the *center* of the dish. HUVECs were stained with UEA1-

680 FITC. Lumen formation was not clear. (e) Brightfield image of HUVECs

681 cocultured with LFs in fibrin gel near 1 mm glass beads *embedded in* the fibrin

682 gel. We observed lumen formation around beads. (f) Confocal image of HUVECs
683 cocultured with LFs in fibrin gel near 1 mm glass beads (dashed red circle)
684 *embedded in* the fibrin gel. HUVECs were stained with UEA1-FITC. We
685 observed lumen formation around beads. (g) Brightfield image of HUVECs
686 cocultured with LFs in fibrin gel near 1 mm glass beads *placed on* the fibrin gel.
687 We observed lumen formation around beads. (h) Confocal image of HUVECs
688 cocultured with LFs in fibrin gel near 1 mm glass beads *placed on* the fibrin gel.
689 HUVECs were stained with UEA1-FITC. We observed lumen formation around
690 the beads. Scale bars: 100 μm (a–d); 1 mm (f, h).
691

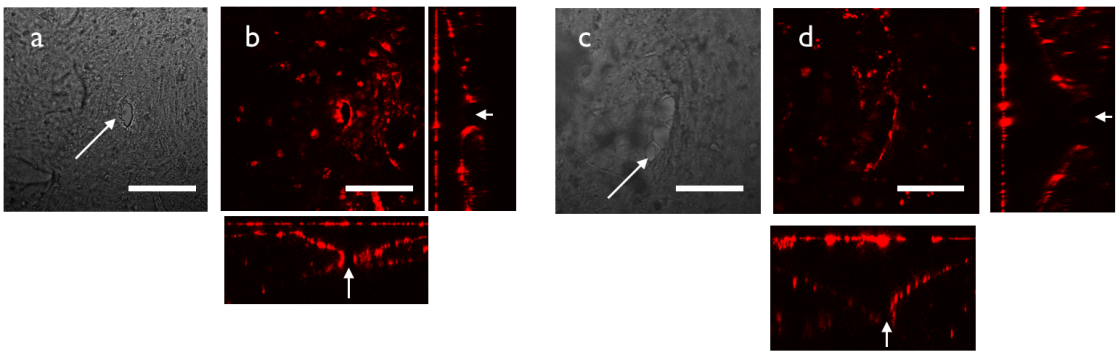

692

693 S3 Fig: Three-dimensional structure of inlet and outlet regions. (a) Brightfield

694 image of the inlet hole region. Arrow: small hole made by fine forceps. (b) Three-

695 dimensional structure of the inlet hole observed by confocal microscopy. We

696 observe RFP-HUVECs covering the hole to make openings to the upper medium

697 reservoir. (c) Brightfield image of the outlet hole region. Arrows indicate a small

698 hole made by fine forceps. Cell debris from the vascular network accumulated near

699 the outlet region (arrowhead). Scale bars: 200 μm.

700

701

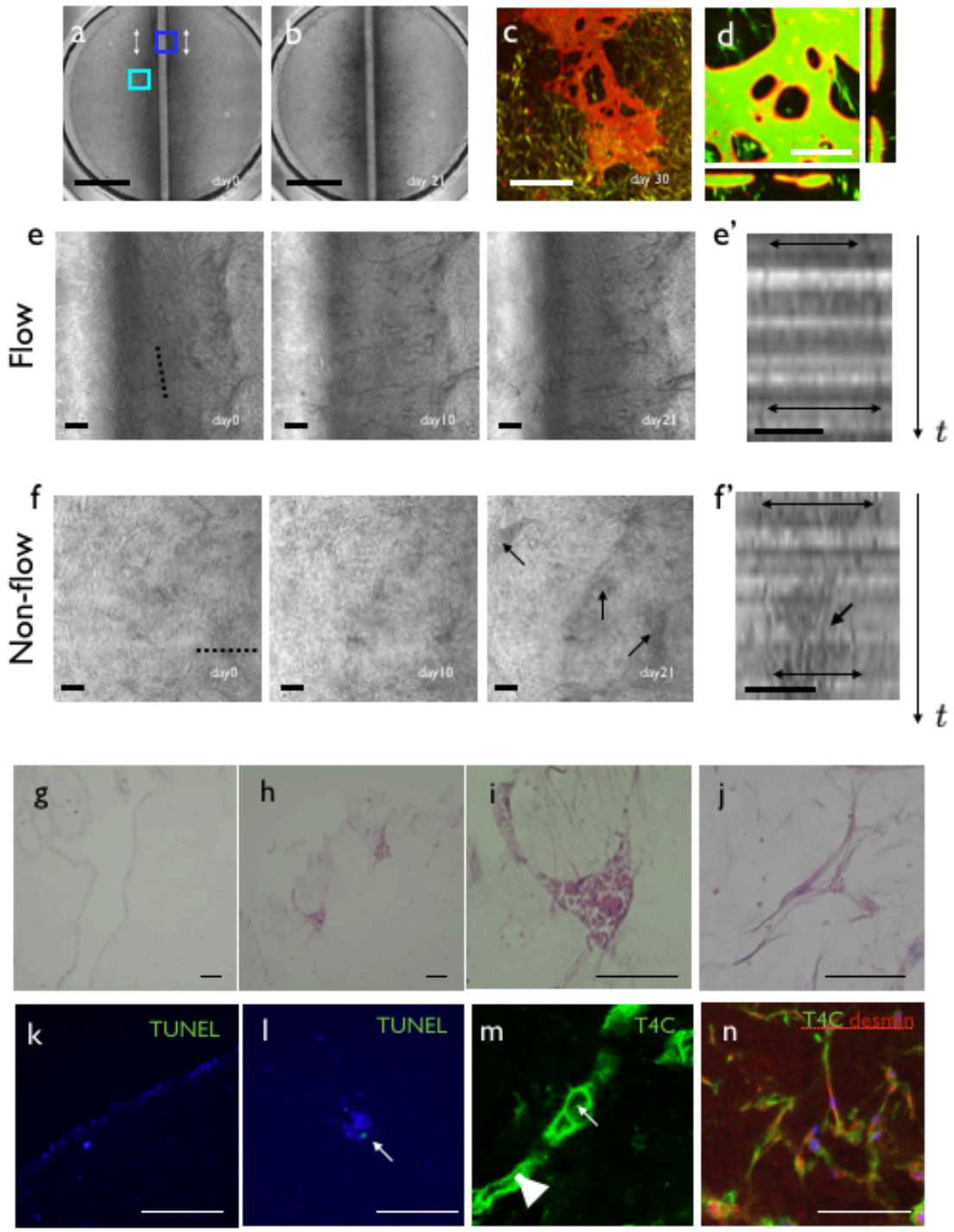

702

703 S4 Fig: Effect of flow on the self-organized endothelial cell network with pericytes.

704 (a) Low magnification view at day 0. Locations of the inlet and outlet are shown
705 by white arrows. (b) Low magnification view at day 21. (c) Confirmation of
706 perfusion at day 30. Endothelial cells were stained with UEA-1 lectin (red) and
707 culture medium with FITC-dextran (green) was perfused. Characteristics of the
708 vessel shape were similar to that without pericytes. (d) Three-dimensional view
709 of the vasculature. We did not observe leakage of FITC-dextran. (e) High
710 magnification view of the flow region [blue box in (a)]. Note that vascular regions
711 increased gradually. (e') Kymograph of the vascular region [dotted line in (e)].
712 Note that the vascular diameter increased gradually (double-headed arrows). (f).
713 High magnification view of the non-flow region [cyan box in (a)]. The vascular
714 region decreased gradually with cell debris inside the vascular lumen (double-
715 headed arrows). (f') Kymograph of vascular region [dotted line in (f)]. Vascular
716 diameter decreased gradually and debris accumulated inside the endothelial cyst
717 (double-headed arrows). (g) Histological observation of the flow region. (h)
718 Histological observation of the low flow region. (i) High magnification view of the
719 cyst structure in the non-flow region. (j) Histological structure of pericytes within

720 a gel in the non-flow region. (k) TUNEL staining of the flow region. No dead cells
721 were observed. (l) TUNEL staining of the non-flow region. A positive signal was
722 observed within the cyst. (m) Type IV collagen staining near the cyst. A large
723 ECM sheath structure was observed (arrowhead) near the cyst (arrow). (n) Type
724 IV collagen and desmin staining of the non-flow region. Desmin-positive pericytes
725 were observed within the gel, which colocalized with type IV collagen. Scale bars:
726 3 mm (a, b); 1 mm (c); 250 μm (d);100 μm (e, f).
727

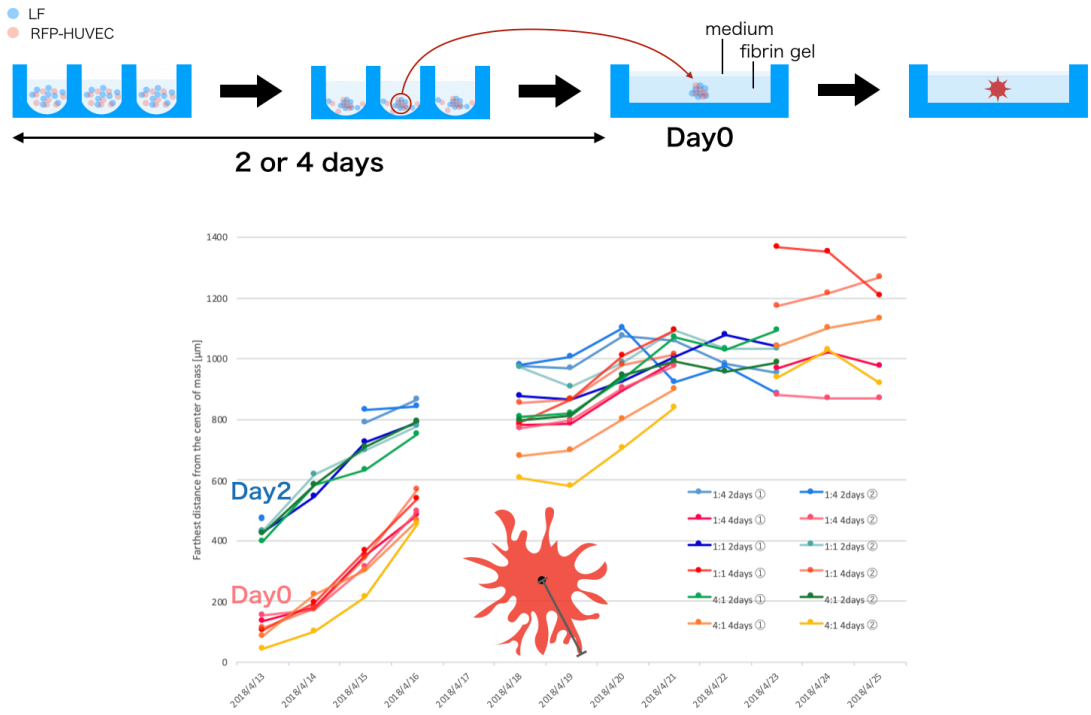

728

729 S5 Fig: Quantification of the sprout length from endothelial cell-containing

730 spheroids. Spheroids containing RFP-HUVECs were cultivated for 2 or 4 days in

731 a culture plate and then transferred to fibrin gel. The length of angiogenic sprouts

732 from the centroid of the fluorescent signal was measured every day. The length of

733 the sprout became saturated after 7 days, and the radius was around 1 mm, which

734 enabled us to directly cut the tip of the sprout to generate an open end.

735

736

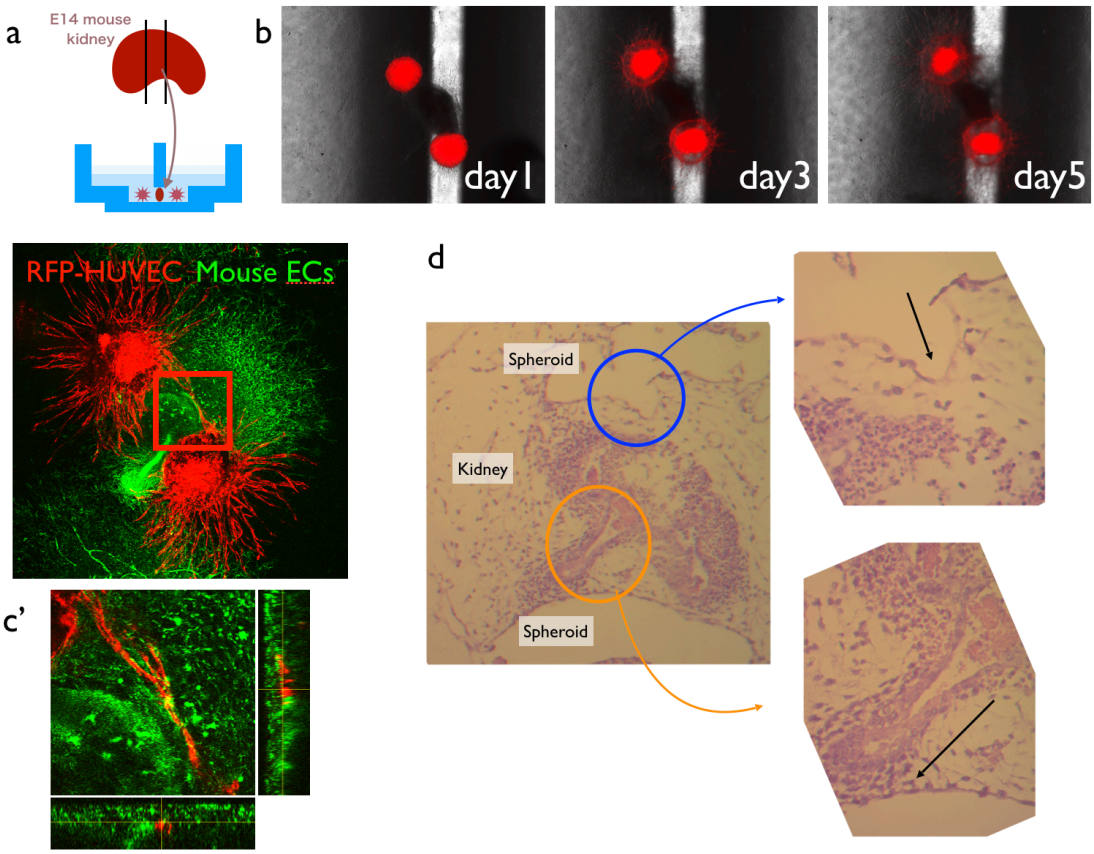

737

738 S6 Fig: Attempt to connect vasculature to the embryonic tissue. (a) E12 mouse

739 embryonic kidney tissue was dissected, and the central one-third of the kidney was

740 embedded in fibrin gel. The tissue was sandwiched by two RFP-HUVEC:hLF

741 spheroids. (b) After 1 week, HUVEC-LF spheroids generated sprouts towards the

742 embryonic kidney tissue. (c) Sprouts from RFP-HUVECs appeared to avoid the

743 embryonic tissue. (c') 3D observation of HUVECs and mouse endothelial cells

744 revealed that, although mouse endothelial cells (green) tended to attach to RFP-

745 HUVECs, they did not connect vasculature with lumens together. (d) Histological

746 observation of the cultured tissue. Kidney explants formed collecting tubule-like

747 structures, but the endothelial sprouts from the HUVEC spheroids did not form a

748 connection with the kidney structure.

749

750 Supporting movie S1: Flow of fluorescent particles in the self-organized capillary
751 network.

752 Real-time movie of fluorescent particles flowing in a synthetic vascular network in
753 fibrin gel.

754

755 Supporting movie S2: Flow of red blood cells in the self-organized capillary network.

756 Real-time movie of red blood cell flowing in a synthetic vascular network in fibrin
757 gel. Blood was diluted 20× using EGM-2 and loaded on one side of the well (Fig.
758 1k,l).

759

760 Supporting movie S3: Cell debris flowing during the medium change (long-term
761 perfusion experiment).

762 Real-time movie of cell debris flowing in a synthetic vascular network in fibrin gel
763 during the long-term perfusion experiment (Fig. 2). We confirmed perfusion
764 during the medium change process.

765

766 Supporting movie S4: dilation of the vessels in the flow region

767 Time-lapse movie of the flow region in the long-term flow experiment (Fig. 3d).

768 The vessel with flow was maintained alive, and some vessels became dilated.

769 Frame rate: 1 day/frame, 30 days.

770

771 Supporting movie S5: Disappearance of unused vessels in the non-flow region.

772 Time-lapse movie of the non-flow region in the long-term flow experiment (Fig.

773 3e). The vessel became disconnected and degraded gradually. Frame rate: 1

774 day/frame, 30 days.

775

776 Supporting movie S6: Movement of pericytes in the flow region

777 Time-lapse movie of pericytes (green) in the flow region (upper half) and non-

778 flow region (lower half). In the flow region, the pericytes simply disappeared,

779 whereas in the non-flow region, pericytes proliferated extensively.

780

781

782 Supporting movie S7: Flow of HL60 cells in the self-organized vascular network.

783 Time-lapse movie of HL60 (green) in HUVEC-RFP vascular network.

784

785

References

1. Gilbert SF, Michael J. Barresi. Developmental Biology. 11th ed. Sinauer; 2018.

2. Wolpert L, Tickle C. Principles of development. 4th ed. New York, New York, USA: Oxford University Press; 2011.

3. Sadler TW. Langman's Medical Embryology. 10th ed. Baltimore: Lippincott Williams & Wilkins; 2006. doi:10.1097/00006534-198801000-00024

4. Shamir ER, Ewald AJ. Three-dimensional organotypic culture: Experimental models of mammalian biology and disease [Internet]. Nature Reviews Molecular Cell Biology. 2014. pp. 647–664. doi:10.1038/nrm3873

5. Clevers H. Modeling Development and Disease with Organoids. Cell. 2016;165: 1586–1597. doi:10.1016/j.cell.2016.05.082

6. Miura T, Yokokawa R. Tissue culture on a chip: Developmental biology

applications of self-organized capillary networks in microfluidic devices. Development Growth and Differentiation. 2016. pp. 505–515. doi:10.1111/dgd.12292

7. Auger FA, Gibot L, Lacroix D. The Pivotal Role of Vascularization in Tissue Engineering. Annu Rev Biomed Eng. 2013;15: 177–200. doi:10.1146/annurev-bioeng-071812-152428

8. Kubota Y, Kleinman HK, Martin GR, Lawley TJ. Role of laminin and basement membrane in the morphological differentiation of human endothelial cells into capillary-like structures. J Cell Biol. 1988;107: 1589–1598. doi:10.1083/jcb.107.4.1589

9. Armulik A, Abramsson A, Betsholtz C. Endothelial/pericyte interactions. Circ Res. 2005;97: 512–523. doi:10.1161/01.RES.0000182903.16652.d7

10. Wagner DD, Frenette PS. The vessel wall and its interactions. Blood. 2008;111: 5271–5281. doi:10.1182/blood-2008-01-078204

11. Williams MR, Azcutia V, Newton G, Alcaide P, Luscinskas FW. Emerging mechanisms of neutrophil recruitment across endothelium [Internet].

818 Trends in Immunology. 2011. pp. 461–469. doi:10.1016/j.it.2011.06.009

819 12. Gupta GP, Massagué J. Cancer Metastasis: Building a Framework

820 [Internet]. Cell. 2006. pp. 679–695. doi:10.1016/j.cell.2006.11.001

821 13. Song HHG, Rumma RT, Ozaki CK, Edelman ER, Chen CS. Vascular

822 Tissue Engineering: Progress, Challenges, and Clinical Promise. Cell Stem

823 Cell. 2018;22: 340–354. doi:10.1016/j.stem.2018.02.009

824 14. Kim S, Lee H, Chung M, Jeon NL. Engineering of functional, perfusable

825 3D microvascular networks on a chip. Lab Chip. 2013;13: 1489–1500.

826 doi:10.1039/c3lc41320a

827 15. Nashimoto Y, Hayashi T, Kunita I, Nakamasu A, Torisawa Y, Nakayama

828 M, et al. Integrating perfusable vascular networks with a three-

829 dimensional tissue in a microfluidic device. Integr Biol. 2017;9: 506–518.

830 doi:10.1039/C7IB00024C

831 16. Nashimoto Y, Okada R, Hanada S, Arima Y, Nishiyama K, Miura T, et al.

832 Vascularized cancer on a chip: The effect of perfusion on growth and drug

833 delivery of tumor spheroid. Biomaterials. 2020;229: 119547.

834 doi:10.1016/j.biomaterials.2019.119547

835 17. van Duinen V, Zhu D, Ramakers C, van Zonneveld AJ, Vulto P,
836 Hankemeier T. Perfused 3D angiogenic sprouting in a high-throughput in
837 vitro platform. Angiogenesis. 2019;22: 157–165. doi:10.1007/s10456-018-
838 9647-0

839 18. Nakatsu MN, Sainson RCA, Aoto JN, Taylor KL, Aitkenhead M, Pérez-
840 del-Pulgar S, et al. Angiogenic sprouting and capillary lumen formation
841 modeled by human umbilical vein endothelial cells (HUVEC) in fibrin
842 gels: The role of fibroblasts and Angiopoietin-1. Microvasc Res. 2003;66:
843 102–112. doi:10.1016/S0026-2862(03)00045-1

844 19. Corbett TH, Griswold DP, Roberts BJ, Peckham JC, Schabel FM. Tumor
845 induction relationships in development of transplantable cancers of the
846 colon in mice for chemotherapy assays, with a note on carcinogen
847 structure. Cancer Res. 1975;35: 2434–9.

848 20. Schneider CA, Rasband WS, Eliceiri KW. NIH Image to ImageJ: 25 years
849 of image analysis. Nat Methods. 2012; doi:10.1038/nmeth.2089

850 21. Schindelin J, Arganda-Carreras I, Frise E, Kaynig V, Longair M, Pietzsch
851 T, et al. Fiji: An open-source platform for biological-image analysis.
852 Nature Methods. 2012. pp. 676–682. doi:10.1038/nmeth.2019
853 22. Sato Y, Poynter G, Huss D, Filla MB, Czirok A, Rongish BJ, et al.
854 Dynamic analysis of vascular morphogenesis using transgenic quail
855 embryos. PLoS One. 2010;5: 1–12. doi:10.1371/journal.pone.0012674
856 23. Ostrowski MA, Huang NF, Walker TW, Verwijlen T, Poplawski C, Khoo
857 AS, et al. Microvascular endothelial cells migrate upstream and align
858 against the shear stress field created by impinging flow. Biophys J.
859 2014;106: 366–374. doi:10.1016/j.bpj.2013.11.4502
860 24. Hsu PP, Li S, Li YS, Usami S, Ratcliffe A, Wang X, et al. Effects of flow
861 patterns on endothelial cell migration into a zone of mechanical
862 denudation. Biochem Biophys Res Commun. 2001;285: 751–759.
863 doi:10.1006/bbrc.2001.5221
864 25. Uemura A, Ogawa M, Hirashima M, Fujiwara T, Koyama S, Takagi H, et
865 al. Recombinant angiopoietin-1 restores higher-order architecture of

growing blood vessels in mice in the absence of mural cells. J Clin Invest. 2002;110: 1619–1628. doi:10.1172/JCI200215621.Introduction

26. Shibue T, Brooks MW, Fatih Inan M, Reinhardt F, Weinberg RA. The outgrowth of micrometastases is enabled by the formation of filopodium-like protrusions. Cancer Discov. 2012;2: 706–721. doi:10.1158/2159-8290.CD-11-0239

27. Davis GE, Stratman AN, Sacharidou A, Koh W. Molecular Basis for Endothelial Lumen Formation and Tubulogenesis During Vasculogenesis and Angiogenic Sprouting. International Review of Cell and Molecular Biology. 2011. pp. 101–165. doi:10.1016/B978-0-12-386041-5.00003-0

28. Newman AC, Chou W, Welch-Reardon KM, Fong AH, Popson SA, Phan DT, et al. Analysis of stromal cell secretomes reveals a critical role for stromal cell-derived hepatocyte growth factor and fibronectin in angiogenesis. Arterioscler Thromb Vasc Biol. 2013;33: 513–522. doi:10.1161/ATVBAHA.112.300782

29. Newman AC, Nakatsu MN, Chou W, Gershon PD, Hughes CCW. The

882 requirement for fibroblasts in angiogenesis: fibroblast-derived matrix
883 proteins are essential for endothelial cell lumen formation. Mol Biol Cell.
884 2011;22: 3791–3800. doi:10.1091/mbc.e11-05-0393
885 30. Sunyer R, Conte V, Escribano J, Elosegui-Artola A, Labernadie A, Valon
886 L, et al. Collective cell durotaxis emerges from long-range intercellular
887 force transmission. Science (80-). 2016;353: 1157–1161.
888 doi:10.1126/science.aaf7119
889 31. Gerhardt H, Golding M, Fruttiger M, Ruhrberg C, Lundkvist A,
890 Abramsson A, et al. VEGF guides angiogenic sprouting utilizing
891 endothelial tip cell filopodia. J Cell Biol. 2003;161: 1163–1177.
892 doi:10.1083/jcb.200302047
893 32. Kourembanas S, Hannan RL, Faller D V. Oxygen tension regulates the
894 expression of the platelet-derived growth factor-B chain gene in human
895 endothelial cells. J Clin Invest. 1990;86: 670–674. doi:10.1172/JCI114759
896